# Activation-induced substrate engagement in ERK signaling

Sayantanee Paul[a,†], Liu Yang[a,b,†], Henry Mattingly[b,c], Yogesh Goyal[b,c,‡], Stanislav Y. Shvartsman[b,c,d], and Alexey Veraksa[a,*]

[a]Department of Biology, University of Massachusetts, Boston, Boston, MA 02125; [b]Lewis-Sigler Institute for Integrative Genomics, [c]Department of Chemical and Biological Engineering, and [d]Department of Molecular Biology, Princeton University, Princeton, NJ 08544

**ABSTRACT** **The extracellular signal-regulated kinase (ERK) pathway is an essential component of developmental signaling in metazoans. Previous models of pathway activation suggested that dissociation of activated dually phosphorylated ERK (dpERK) from MAPK/ERK kinase (MEK), a kinase that phosphorylates ERK, and other cytoplasmic anchors, is sufficient for allowing ERK interactions with its substrates. Here, we provide evidence for an additional step controlling ERK's access to substrates. Specifically, we demonstrate that interaction of ERK with its substrate Capicua (Cic) is controlled at the level of ERK phosphorylation, whereby Cic binds to dpERK much stronger than to unphosphorylated ERK, both in vitro and in vivo. Mathematical modeling suggests that the differential affinity of Cic for dpERK versus ERK is required for both down-regulation of Cic and stabilizing phosphorylated ERK. Preferential association of Cic with dpERK serves two functions: it prevents unproductive competition of Cic with unphosphorylated ERK and contributes to efficient signal propagation. We propose that high-affinity substrate binding increases the specificity and efficiency of signal transduction through the ERK pathway.**

**Monitoring Editor**
Alex Mogilner
New York University

Received: Jul 3, 2019
Revised: Dec 16, 2019
Accepted: Dec 21, 2019

## INTRODUCTION

The extracellular signal-regulated kinase (ERK) is the final component of the Raf-MAPK/ERK kinase-ERK (Raf-MEK-ERK) signaling module, which functions downstream of receptor tyrosine kinases (RTKs) and controls multiple cellular processes, including cell proliferation and differentiation (Lemmon and Schlessinger, 2010; Futran *et al.*, 2013). Activated dually phosphorylated ERK (dpERK) relays pathway activation to the cell via phosphorylation of multiple substrates (Futran *et al.*, 2013). ERK interactions with substrates are typically mediated by two docking domains, the D-site recruitment site (DRS, also known as the common docking, or CD domain), which binds the conserved D-site motif in the substrates, and the F-site recruitment site (FRS), which binds to the substrates containing the FXF motif (also known as the DEF motif) (Jacobs *et al.*, 1999; Sharrocks *et al.*, 2000; Tanoue *et al.*, 2000; Futran *et al.*, 2013).

To understand how ERK carries out its multiple cellular functions, it is critical to establish how pathway activation affects the ability of ERK to recognize its substrates. It is thought that unphosphorylated ERK is sequestered in the cytoplasm by MEK and other cytosolic scaffold and anchor proteins (Roskoski, 2012). Phosphorylation of ERK by MEK results in the release of dpERK from complexes with MEK and other cytoplasmic anchors, enabling subsequent association with substrates in the nucleus and the cytoplasm (Fukuda *et al.*, 1997; Adachi *et al.*, 1999). Whether ERK activation contributes to substrate selection is not well understood. It has been proposed that formation of dpERK results in a conformational change that allows binding of the FRS motif in ERK to the FXF motif in substrate proteins such as ELK1 (Lee *et al.*, 2004). However, a subsequent study found that ERK phosphorylation results in reduced binding to ELK1 (Burkhard *et al.*, 2011).

This article was published online ahead of print in MBoC in Press (http://www.molbiolcell.org/cgi/doi/10.1091/mbc.E19-07-0355) on January 8, 2020.

†These authors contributed equally to this work.

‡Present address: Department of Bioengineering, University of Pennsylvania, Philadelphia, PA 19104.

*Address correspondence to: Alexey Veraksa (alexey.veraksa@umb.edu).

Abbreviations used: Cic, Capicua; dpERK, dually phosphorylated ERK; DRS, D-site recruitment site; ERK, extracellular signal-regulated kinase; FRS, F-site recruitment site; IgG, immunoglobulin G; IPTG, isopropyl β-D-1-thiogalactopyranoside; MAPK, mitogen-activated protein kinase; MEK, MAPK/ERK kinase; RTK, receptor tyrosine kinase; SBP, streptavidin binding peptide; *Sem*, *Sevenmaker*.

One of the key ERK targets in *Drosophila* and mammals is the high mobility group–box transcriptional repressor Capicua (Cic), which controls tissue patterning and organ growth (Jimenez *et al.*, 2000; Astigarraga *et al.*, 2007; Tseng *et al.*, 2007; Ajuria *et al.*, 2011; Grimm *et al.*, 2012; Lim *et al.*, 2013; Jin *et al.*, 2015; Yang and Veraksa, 2017). In *Drosophila*, Cic phosphorylation and down-regulation is involved in most developmental contexts that are under ERK control (Jimenez *et al.*, 2012). In humans, mutations in CIC have been implicated in the neurodegenerative disease spinocerebellar ataxia type 1 (Lam *et al.*, 2006; Fryer *et al.*, 2011) and in the majority of oligodendroglioma cases, as well as other cancers (Simon-Carrasco *et al.*, 2017; Tanaka *et al.*, 2017; Tan *et al.*, 2018). In all contexts studied so far in *Drosophila*, Cic functions as a transcriptional repressor whose activity is inhibited in response to ERK activation (Jimenez *et al.*, 2012). Recent evidence suggests that Cic phosphorylation by ERK leads to rapid relief of repression through interference with DNA binding or interactions with corepressors, followed by slower export from the nucleus and eventual proteolytic degradation (Astigarraga *et al.*, 2007; Grimm *et al.*, 2012; Lim *et al.*, 2013, 2015). Because all of the proposed modes of Cic inactivation are dependent on the ERK-mediated phosphorylation of Cic, it is essential to determine how ERK associates with Cic. Previous studies identified a region in *Drosophila* Cic (the C2 motif) that mediates its binding to ERK (Astigarraga *et al.*, 2007; Futran *et al.*, 2015); however, these studies used the inactive (unphosphorylated) form of ERK.

Here, we report that Cic interacts with activated, dually phosphorylated ERK with a much higher affinity compared with unphosphorylated ERK. Our data suggest that preferential Cic-dpERK interaction prevents unproductive competition of Cic with unphosphorylated ERK, when both Cic and ERK are localized in the same cellular compartment. Furthermore, higher affinity of Cic for dpERK may be required for efficient signal propagation, as it contributes to pathway output (down-regulation of Cic) and increases the steady-state level of dpERK. Based on this, we propose that activation-dependent association with Cic is an integral part of ERK signaling dynamics that serves as an additional checkpoint to regulate the specificity and efficiency of signal propagation.

## RESULTS AND DISCUSSION

### ERK activation is required and sufficient for high-affinity interaction with Cic

Previous studies of interactions between ERK and Cic used unphosphorylated forms of ERK in binding experiments (Astigarraga *et al.*, 2007; Futran *et al.*, 2015). For testing whether activation of ERK affects its interaction with Cic, V5-tagged Cic (Cic-V5) expressed in *Drosophila* S2 cells was immobilized on streptavidin beads and incubated with bacterially expressed, purified rat ERK2, which was converted into the active form by coexpression with active MEK (Figure 1A). ERK2 phosphorylation resulted in a much more robust interaction with Cic (Figure 1A). We observed a similar result with the fly ERK protein using extracts from S2 cells expressing either *Drosophila* ERK alone or ERK in combination with MEK and Raf, which is sufficient to induce dpERK formation (Tipping *et al.*, 2010), and streptavidin binding peptide (SBP)-tagged Cic (Figure 1B). Activation of ERK by MEK by dual phosphorylation is therefore sufficient to convert it into a form that has a higher affinity for Cic compared with unphosphorylated ERK.

To determine whether full activation of ERK is required for its increased affinity for Cic, we studied ERK/Cic binding using the T198A and Y200F ERK mutants that disrupt the TEY phosphorylation motif targeted by MEK (Canagarajah *et al.*, 1997). As shown in Figure 1C, mutation of either residue impaired the binding between Cic and *Drosophila* ERK-Flag when both were coexpressed in S2 cells, relative to the wild-type enzyme, suggesting that full ERK activation and formation of dpERK is required for its highest affinity for Cic. We note that in this experiment coexpression of ERK with Cic resulted in the stabilization of the activated form of ERK, likely due to the effect of shielding of dpERK from the action of phosphatases in the Cic-dpERK complex (Kim *et al.*, 2011). Collectively, these studies reveal that ERK phosphorylation is required and sufficient to induce a high-affinity interaction with Cic (Figure 1D).

### Preferential binding of Cic to dpERK in vivo

To determine whether Cic preferentially associates with dpERK in vivo, we studied the binding between Cic-Venus (Grimm *et al.*, 2012), which is expressed from genomic regulatory sequences at the endogenous level, and the endogenous ERK protein in 0- to 4-h *Drosophila* embryos. At this stage, dpERK is formed specifically at the embryonic termini downstream of RTK Torso activation (Gabay *et al.*, 1997). Immunoprecipitation of Cic-Venus resulted in copurification of endogenous ERK, which also gave a strong dpERK signal (Figure 2A). To test whether dpERK is limiting in this assay, we generated additional dpERK via maternal expression of a dominant-active form of MEK, $MEK^{E203K}$ (Goyal *et al.*, 2017a). In these embryos, dpERK was produced throughout the embryo, including the middle region, where dpERK is normally absent (Figure 2, B and C), while the total ERK level was unchanged (Figure 2A and Supplemental Figure S1). Remarkably, under these conditions, a higher amount of total ERK was associated with Cic-Venus, consistent with a higher overall level of dpERK in these embryos (Figure 2A). We note that the level of Cic-Venus was lower in $MEK^{E203K}$-overexpressing embryos (Figure 2A, GFP signal), likely because of excessive degradation due to ERK hyperactivity (Goyal *et al.*, 2017b). However, we still observed an increase in the amount of total ERK in our coimmunoprecipitation experiment, despite it being pulled down by this lower amount of Cic-Venus. In summary, Cic has a higher affinity for dpERK in vivo, and the amount of ERK bound to Cic is limited by the level of dpERK produced downstream of RTK activation.

### Preferential association of Cic with dpERK prevents competition with ERK and contributes to efficient signal propagation

Previous quantitative models of dpERK interactions with substrates assumed that dpERK is largely nuclear (Kim *et al.*, 2011). However, several studies showed that both Cic and dpERK can localize in the cytoplasm in developing tissues (Roch *et al.*, 2002; Astigarraga *et al.*, 2007; Coppey *et al.*, 2008; Grimm *et al.*, 2012). We studied ERK and Cic localization in *Drosophila* cultured S2 cells under the basal conditions of limited ERK phosphorylation or in cotransfection with Raf and MEK, which generates large amounts of dpERK (Tipping *et al.*, 2010). Transfection of Cic alone resulted in a predominantly cytoplasmic localization, with some nuclear signal (Figure 3, A–A″). Cotransfection of ERK with Raf and MEK led to the formation of dpERK, which was also localized mostly in the cytoplasm (Figure 3, B–B‴). Upon cotransfection of Cic with ERK, Raf, and MEK, the Cic and dpERK signals were still primarily cytoplasmic, with detectable but low nuclear staining (Figure 3, C–C‴). These data showed that Cic, ERK, and dpERK can coexist in the cytoplasm in S2 cells, which agrees with previously reported localization of Cic and dpERK in both the nucleus and the cytoplasm in vivo (Roch *et al.*, 2002; Astigarraga *et al.*, 2007; Coppey *et al.*, 2008; Grimm *et al.*, 2012). Subcellular localization of the two major ERK phosphatases in

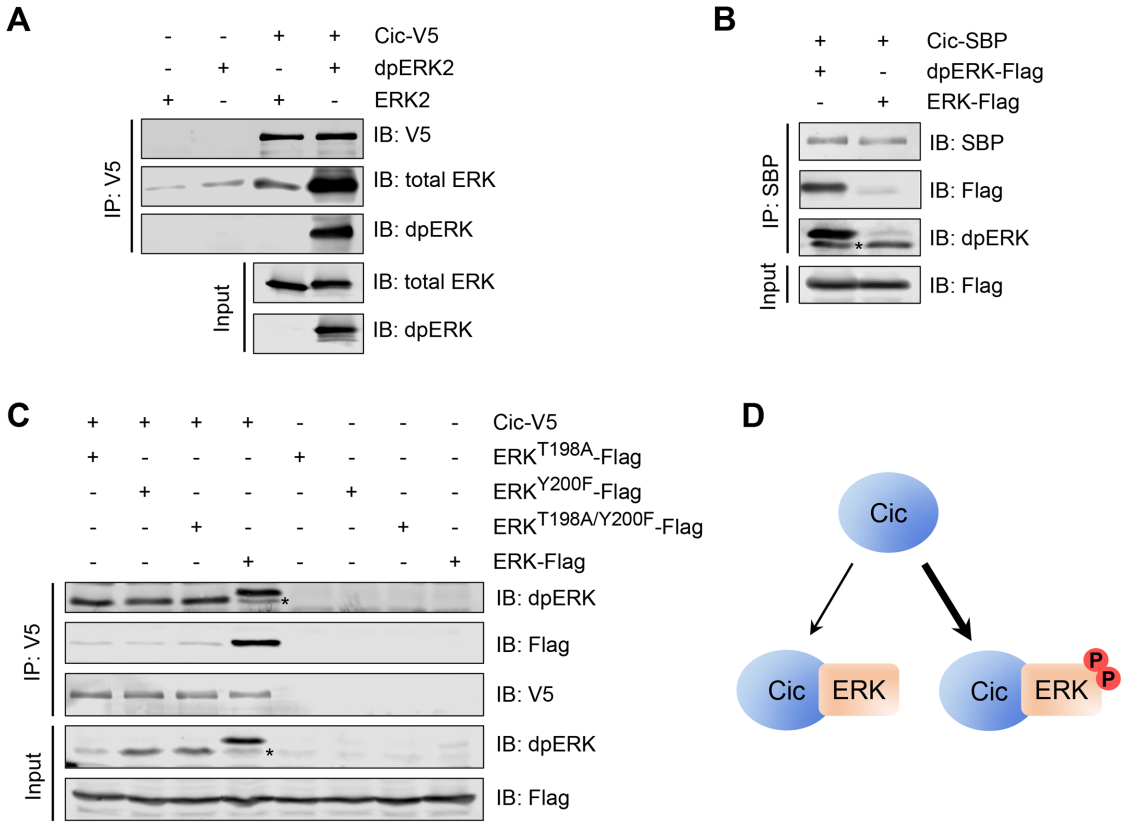


FIGURE 1: ERK phosphorylation in the activation loop is required and sufficient to induce strong binding to Cic. (A) An in vitro binding assay in which bacterially expressed purified rat ERK2 and dpERK2 were incubated with beads bound with Cic-V5 purified from S2 cells, analyzed by Western blotting. Cic-V5 strongly prefers dpERK2 over unphosphorylated ERK2. (B) An in vitro binding assay in which protein lysates from S2 cells cotransfected with *Drosophila* ERK-Flag, Raf, and MEK (dpERK-Flag) or transfected only with ERK-Flag were incubated with beads bound with separately expressed Cic-SBP, analyzed by Western blotting. Cic-SBP strongly prefers dpERK over unphosphorylated ERK. (C) Coimmunoprecipitation between Cic and ERK mutants in *Drosophila* S2 cells, analyzed by Western blotting with the indicated antibodies. Blocking the formation of dually phosphorylated ERK (dpERK) results in a lower affinity for Cic. Asterisks in B and C indicate endogenous (untagged) dpERK present in S2 cells. (D) Summary of Cic interactions with ERK and dpERK. Cic preferentially associates with dpERK.

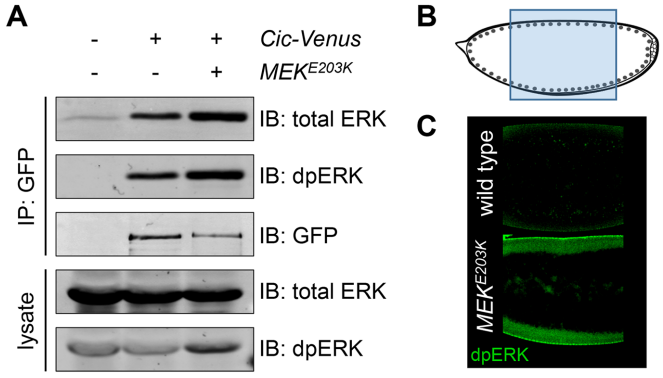


FIGURE 2: Cic preferentially associates with dpERK in vivo. (A) Extracts from embryos expressing Cic-Venus alone or Cic-Venus with activated MEK ($MEK^{E203K}$) were immunoprecipitated with anti–green fluorescent protein (GFP) beads and analyzed by Western blotting. Up-regulation of ERK signaling is sufficient to increase ERK association with Cic in vivo. (B, C) Overexpression of activated MEK ($MEK^{E203K}$) results in an increase of dpERK formation in the middle of the embryo. (B) Schematic diagram of the embryo, indicating the location of the images shown in C.

*Drosophila* is consistent with the importance of cytoplasmic regulation of dpERK: both Mkp3 and PTP-ER are cytoplasmic proteins (Karim and Rubin, 1999; Molnar and de Celis, 2013).

We hypothesized that preferential association of Cic with dpERK may be important for preventing competition between ERK and dpERK for binding to Cic, when both ERK forms and Cic are localized in the same cellular compartment (cytoplasm). Such competition would occur if ERK was still present in significant amount after pathway activation. To determine whether the production of dpERK in the cells that are cotransfected with ERK, Raf, and MEK is limited, we analyzed extracts from S2 cells expressing ERK alone or ERK together with MEK and RAF by Western blotting with an antibody specific for unphosphorylated ERK (unphospho-ERK). We did not observe a significant down-regulation of the unphospho-ERK signal upon cotransfection with Raf and MEK, despite detecting robust formation of dpERK (Figure 3, D and E), suggesting that dpERK is present in limited amounts in these cells, and unphosphorylated ERK is still the predominant form. We also compared the normalized ratios of unphospho-ERK to total ERK by immunofluorescence of transfected S2 cells. These measurements showed that, upon cotransfection with Raf and MEK, the amount of unphosphorylated ERK was reduced from 1 to

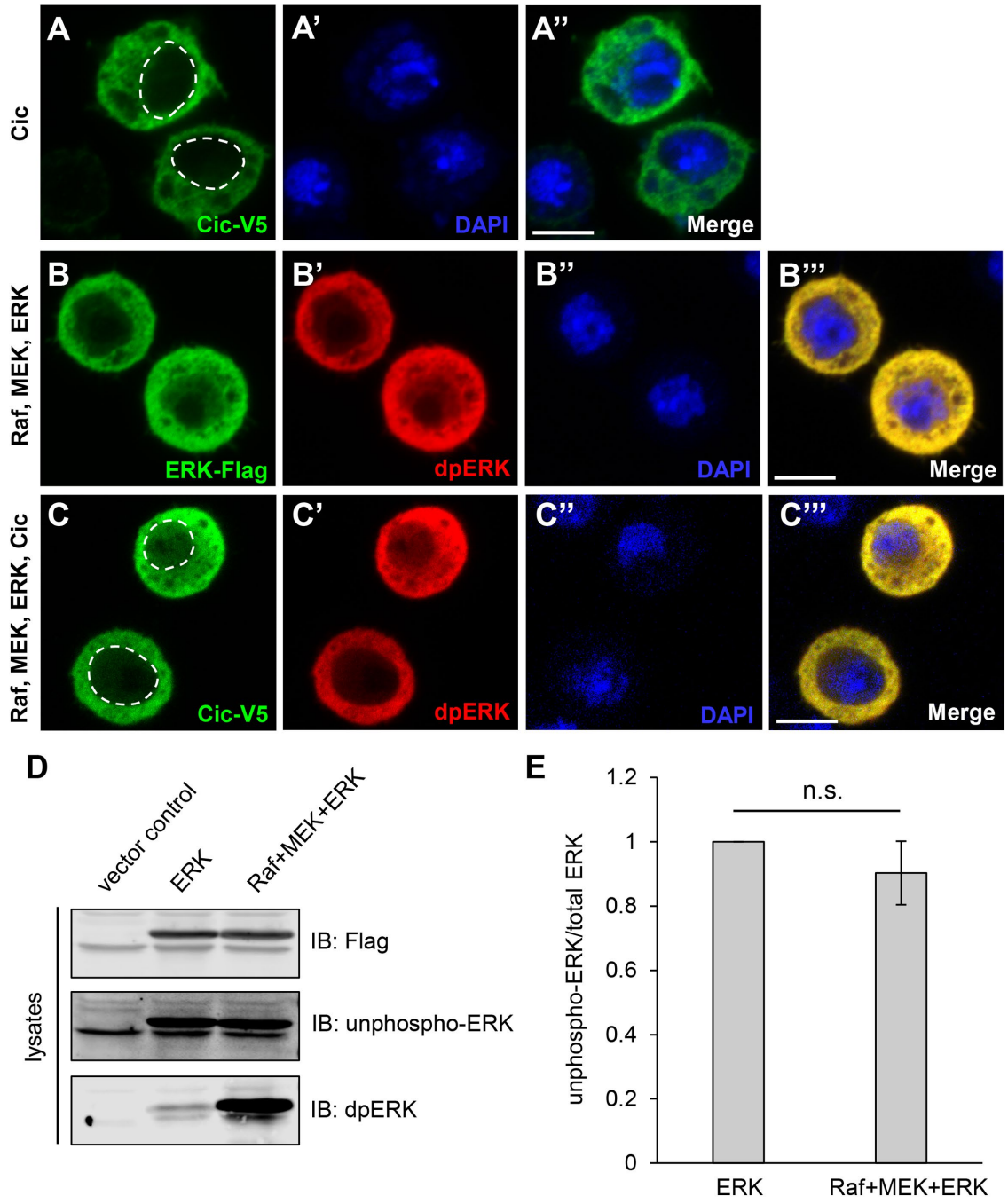


FIGURE 3: Localization studies of Cic, ERK, and dpERK in S2 cells, and ERK phosphorylation analysis. In A–C‴, transfected expression constructs are shown on the left, and staining signals are shown on the individual panels. In A and C, dashed lines indicate nuclear boundaries. Scale bars, 5 μm. (A–A″) Cic-V5 was predominantly cytoplasmic, with some nuclear distribution. (B–B‴) When cotransfected with MEK and Raf, both ERK-Flag and dpERK signals were mostly cytoplasmic but also showed nuclear localization. (C–C‴) When Cic-V5 and ERK-Flag were cotransfected with Raf and MEK, the Cic-V5 and dpERK signals remained predominantly cytoplasmic, with some nuclear distribution. (D) Extracts from S2 cells transfected with vector control, ERK alone, or ERK together with MEK and RAF were analyzed by Western blotting. A representative blot of three independent experiments is shown. (E) Quantification of results in D. No significant down-regulation of unphospho-ERK signal was observed with cotransfection of Raf and MEK, despite a detectable up-regulation of dpERK. $n = 3$; n.s., not significant ($p > 0.05$).

0.75 (a 25% decrease), again indicating only limited dpERK formation in cells (Supplemental Figure S2).

To explore the consequences of colocalization of Cic, ERK, and dpERK, we formulated a mathematical model in which Cic and both the unphosphorylated and phosphorylated forms of ERK are localized in the same compartment (Figure 4A; see Supplemental Materials and Methods for model details). The model describes the conversion of an inactive form of ERK (E) to its active dually phosphorylated form, dpERK (E*), in the presence of active enzyme (MEK) that phosphorylates ERK and phosphatases that

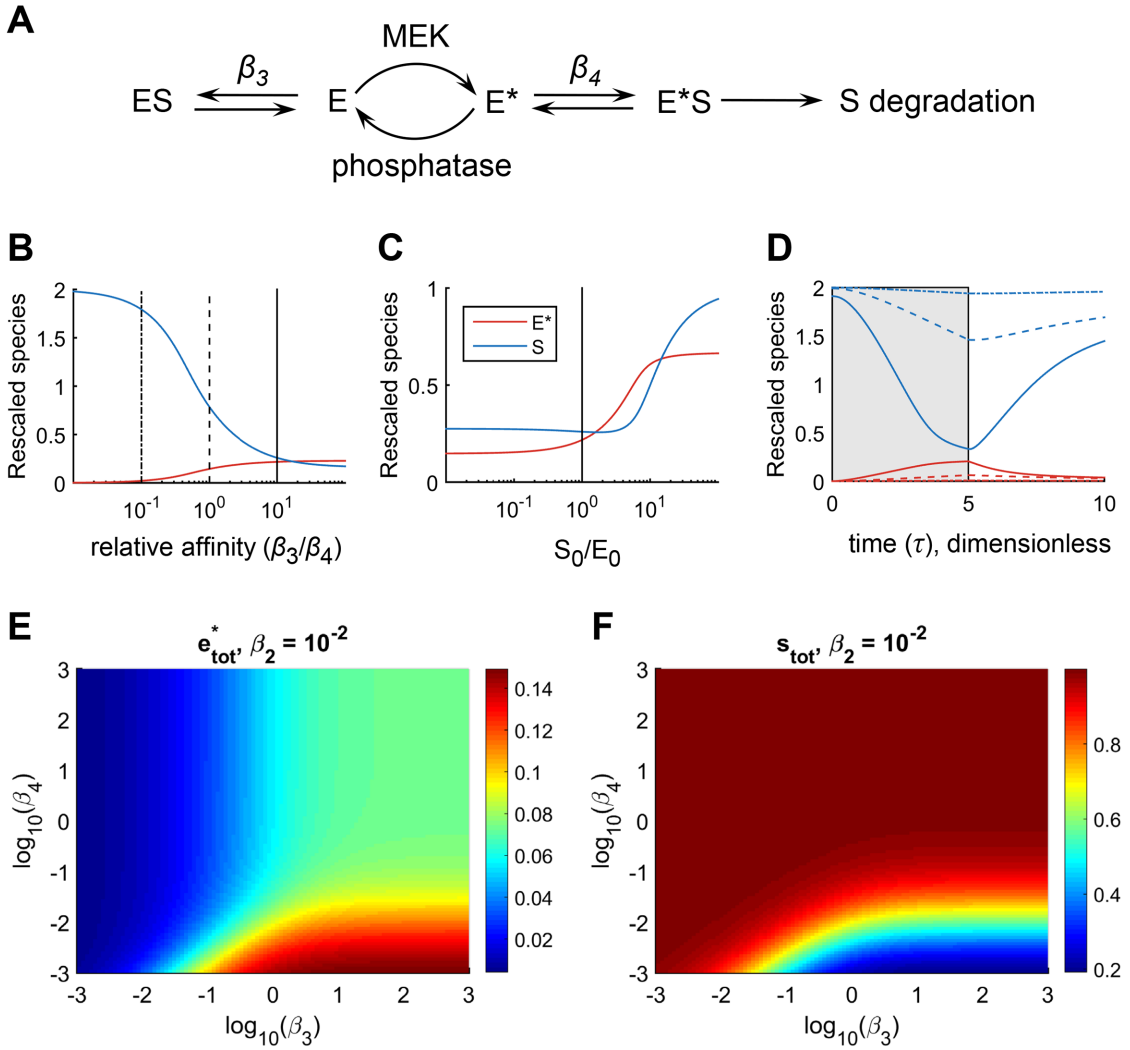


FIGURE 4: Mathematical model of signaling from dpERK (E*) to Cic (S). Simulations were carried out under the conditions of colocalization of Cic, ERK, and dpERK in the same compartment. See text and Supplemental Materials and Methods for model details. (A) Diagram of main reactions. (B) Steady-state concentrations of the total amounts (free and in complexes) of E* and S for various values of $\beta_3$ and $\beta_4$. Smaller $\beta_3$ indicates stronger substrate binding to E, while smaller $\beta_4$ indicates stronger substrate binding to E*. In all panels, $\beta_4 = 10^{-2}$. Strong preferential association of E* with S (large value of $\beta_3/\beta_4$) is required for efficient degradation of S (blue curve) and generation of E* (red curve). (C) Steady-state concentrations of E* and S for different values of $S_0$, the steady-state amount of S in the absence of input to the pathway. Here, $\beta_3 = 10^{-1}$. Low concentrations of S (Cic) result in inefficient formation of E* (dpERK). (D) Transients of E* and S for selected values of $\beta_3$, corresponding to the vertical lines in B ($\beta_3 = 10^{-3}$, $10^{-2}$, and $10^{-1}$). The time courses were initialized from the steady state when there is no input, then at $\tau = 0$, an input was introduced until $\tau = 5$ (gray patch), at which time the input was removed, and the system relaxed back toward the initial steady state. (E, F) Model predictions of the steady-state dependence of $e^*_{tot}$ and $s_{tot}$ on $\beta_3$ and $\beta_4$, for $\beta_2 = 10^{-2}$ and with all other parameters the same as in B and C. Substantial activation of $e^*_{tot}$ and degradation of $s_{tot}$ requires that both $\beta_4 \leq \beta_3$ and $\beta_4 \leq \beta_2$.

dephosphorylate ERK. Active enzyme E* binds to and promotes the degradation of its substrate (S), which is continuously synthesized and also undergoes intrinsic degradation when free or in any complex. Inactive enzyme E also binds S, but does not cause its degradation. In this model, an outcome of successful signal propagation is a reduction in the level of S (Figure 4A).

We investigated the effects of the relative strengths of binding of substrate (S) to the inactive (E) and active (E*) forms of enzyme, which are controlled by the binding parameters $\beta_3$ and $\beta_4$, respectively. The $\beta$ parameters in this model are Michaelis–Menten constants rescaled by the total ERK concentration and indicate the concentrations of unmodified ($\beta_3$) or modified ($\beta_4$) enzyme at which unbound substrate concentration falls due to binding or degradation. Therefore, smaller values of $\beta_3$ and $\beta_4$ indicate stronger interactions of Cic with the corresponding form of ERK; that is, smaller $\beta_3$ indicates stronger binding of S to E, whereas smaller $\beta_4$ indicates stronger binding of S to E*. At steady state, varying the ratio of $\beta_3/\beta_4$ revealed that strong preferential association of E* with S (large values of $\beta_3/\beta_4$) is required for efficient substrate down-regulation (Figure 4B, blue curve). In principle, inactive E could interact with S and compete with active E*. However, under this condition, the pathway cannot function efficiently, as shown by an inability of S to be degraded under small values of $\beta_3/\beta_4$

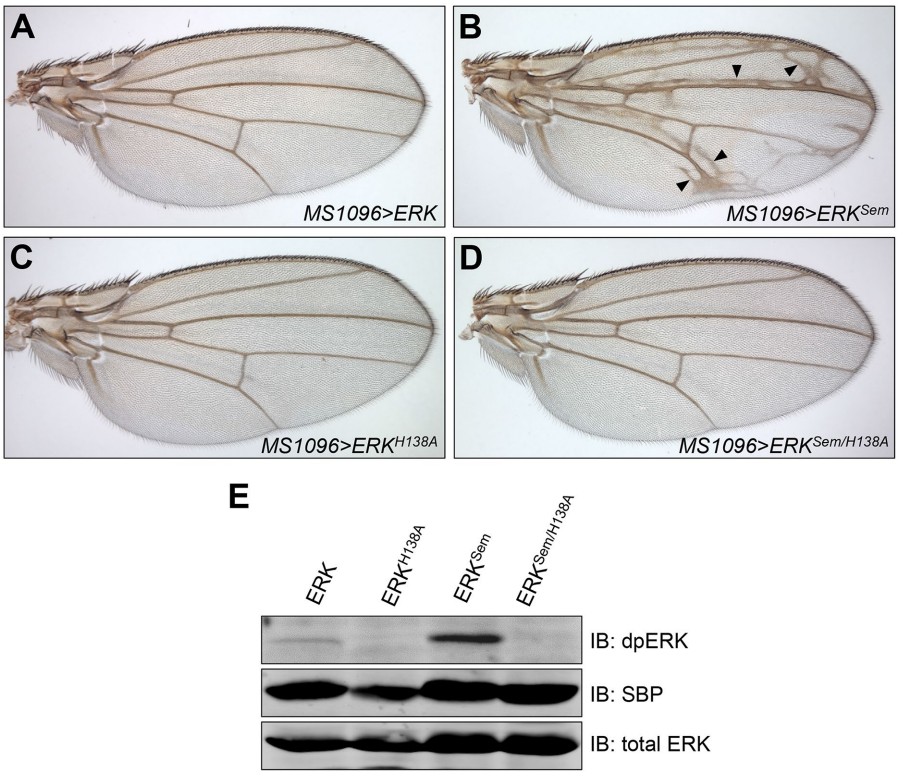


**FIGURE 5:** The H138A mutation *in cis* suppresses the ability of ERK$^{Sem}$ to induce ectopic veins. (A–D) Wings from adult female flies expressing indicated constructs under the control of the *MS1096-GAL4* driver: (A) *UAS-ERK-SBP*, (B) *UAS-ERK$^{Sem}$-SBP*, (C) *UAS-ERK$^{H138A}$-SBP*, and (D) *UAS-ERK$^{Sem/H138A}$-SBP*. Arrowheads in B mark ectopic veins. (E) Western blot showing ERK-SBP and dpERK levels in embryo extracts expressing indicated ERK isoforms under the control of the *da-GAL4* driver.

(Figure 4B, blue curve). Our simulations also showed that preferential association of S with E* is required even for the generation of significant amounts of active enzyme, E* (Figure 4B, red curve). As an extension of this requirement, only a small amount of activated enzyme is generated when concentration of S is low (Figure 4C). Dynamic simulations have confirmed the findings of steady-state analysis: efficient degradation of S and generation of E* was achievable at $\beta_3/\beta_4$ values approaching 10 (Figure 4D). A more complete exploration of the parameter space further confirmed these observations (Figure 4, E and F). Thus, preferential association of Cic with dpERK is required for efficient signal propagation in the presence of significant levels of unphosphorylated ERK, both in terms of the effects of active ERK on substrate degradation and for establishing high levels of ERK activation.

### Cic-ERK interactions are critical for setting dpERK level and signaling in vivo

Given the importance of Cic-ERK interactions for ERK pathway activity, we investigated the effects of disrupting Cic-ERK binding at the level of ERK in vivo. Previous biochemical studies identified specific residues near the DRS domain in mammalian ERK that contribute to its interactions with the C2 domain of *Drosophila* Cic (Futran *et al.*, 2015). One such residue is H123, whose mutation to alanine in mammalian ERK2 reduced the binding affinity to the C2 domain (Futran *et al.*, 2015). This histidine residue is conserved and corresponds to H138 in *Drosophila* ERK. To test for the functional importance of this residue in vivo, we generated SBP-tagged variants of ERK that carried either the single H138A mutation, the activating mutation in the DRS domain, *Sevenmaker* (ERK$^{Sem}$, D334N), which impairs ERK binding to phosphatases (Bott *et al.*, 1994; Brunner *et al.*, 1994; Tanoue *et al.*, 2000), or a combination of H138A and D334N within the same polypeptide. These ERK-SBP variants were expressed in vivo using the wing pouch *MS1096-GAL4* driver (Capdevila and Guerrero, 1994). The development of wing veins is promoted by the activation of the epidermal growth factor receptor and dpERK, which relieves Cic-mediated repression of vein-specific genes and allows vein formation (Roch *et al.*, 2002; Ajuria *et al.*, 2011). Overexpression of wild-type ERK-SBP did not alter the normal venation pattern (Figure 5A), while overexpression of ERK$^{Sem}$-SBP promoted formation of ectopic veins (Figure 5B). This phenotype is likely caused by ectopic inhibition of Cic function by overactive ERK, outside the normal areas of vein formation (Roch *et al.*, 2002; Ajuria *et al.*, 2011). Interestingly, while overexpression of ERK$^{H138A}$-SBP alone did not alter the normal venation pattern (Figure 5C), this mutation in combination with *Sevenmaker* within the same polypeptide (ERK$^{Sem/H138A}$-SBP) strongly suppressed the ability of the double-mutant protein to induce ectopic veins (Figure 5D). Therefore, the H138A mutation is completely dominant over the activating mutation ERK$^{Sem}$, when tested *in cis* within the same protein.

The inability of ERK$^{Sem/H138A}$-SBP to induce ectopic veins might be interpreted solely through loss of binding to Cic, which is expected for the H138A mutation (Futran *et al.*, 2015). However, it is possible that a reduction of binding to Cic would also lead to a reduction in steady-state level of dpERK due to the action of phosphatases (Kim *et al.*, 2011), which would contribute to the inability of the double-mutant protein to induce ectopic veins. To distinguish between these possibilities, we compared steady-state phosphorylation levels of various SBP-tagged ERK mutants. Protein extracts from dissected larval wing disks did not provide sufficient dpERK for analysis on Western blots. We therefore analyzed dpERK levels of the ERK-SBP variants in *Drosophila* embryos using the *da-GAL4* driver, which is expressed ubiquitously. Because all ERK-SBP variants were injected as a matching set into the same genomic location and provided equivalent levels of total ERK (Figure 5E), expression in the embryo can be used as a valid method of comparison of dpERK levels. The level of phosphorylation (dpERK signal) of the ERK$^{Sem}$-SBP protein was much higher than that of the wild-type ERK-SBP or ERK$^{H138A}$-SBP (Figure 5E). Interestingly, the level of phosphorylation of the double-mutant ERK$^{Sem/H138A}$-SBP protein was much lower than that of ERK$^{Sem}$-SBP (Figure 5E). This result reveals two important properties of the mutant ERK proteins. First, it shows that the ERK$^{Sem}$ protein is still susceptible to inactivation by phosphatases, because a reduction in Cic binding due to the H138A mutation resulted in a reduction in steady-state phosphorylation of ERK$^{Sem/H138A}$-SBP. Second, it suggests that the inability of the ERK$^{Sem/H138A}$-SBP protein to induce the ectopic vein phenotype is due to a combination of both reduced binding to Cic and a strong reduction in phosphorylation. These results underscore the importance of Cic-ERK interactions in vivo

and highlight their importance for maintaining high levels of dpERK, which is required for pathway activity (seen here as formation of ectopic wing veins).

### Conclusion

Previous studies have shown that substrates of ERK may have preferences for binding to either the active or the inactive form of ERK (Lee *et al*., 2004; Burkhard *et al*., 2011) and have mapped the dynamic ERK interactome (von Kriegsheim *et al*., 2009). Here, we established that phosphorylated ERK (dpERK) interacts with its substrate Cic more strongly than unphosphorylated ERK. Our data suggest that the preferred binding of Cic to dpERK is functionally important at two levels: first, it prevents a possible competition between ERK and dpERK for binding to Cic, when these proteins are localized in the same cellular compartment; second, it may allow for efficient signal propagation when only a small proportion of ERK is converted to dpERK. In support of the latter, we have shown that only a small fraction of ERK gets phosphorylated upon activation with Raf and MEK in cultured S2 cells (Figure 3 and Supplemental Figure S2), consistent with our previous results in vivo (Johnson *et al*., 2017).

In *Drosophila*, ERK-mediated Cic phosphorylation and down-regulation is involved in most developmental contexts that are under ERK control. *Drosophila* Cic interacts with dpERK through the C2 docking site, which is not well conserved in other species (Astigarraga *et al*., 2007; Futran *et al*., 2015). C2 domain-mediated down-regulation is therefore a unique property of fly Cic; however, the exact mechanism of Cic down-regulation upon dpERK binding is not fully understood. It likely involves phosphorylation of multiple sites in Cic upon binding of dpERK through the C2 domain (S.P., unpublished data). One of the potential mechanisms of Cic down-regulation is proteolytic degradation (Roch *et al*., 2002; Astigarraga *et al*., 2007; Suisse *et al*., 2017). A stronger binding of Cic to dpERK may thus represent a mechanism to ensure efficient phosphorylation and subsequent degradation of Cic, possibly still in the dpERK-bound state. This would ensure that dpERK is available for phosphorylating other substrates like Bicoid and Hunchback during embronic patterning, after Cic protein levels are reduced (Ronchi *et al*., 1993; Löhr *et al*., 2009; Kim *et al*., 2010). We have shown by mathematical modeling that preferential association of Cic with dpERK also contributes to the maintenance of a steady-state level of dpERK, which in turn is required for pathway output (i.e., Cic degradation), which is critical for the patterning of the embryonic termini (Astigarraga *et al*., 2007). Together, our results suggest that activation-induced high-affinity binding of dpERK to Cic is an important part of ERK signaling dynamics that can increase both the specificity and efficiency of signaling.

## MATERIALS AND METHODS

### Expression constructs, cell culture, and immunoprecipitations

Construction of C-terminally tagged full-length *pMT-Cic-V5* and *pMK33-Cic-SBP* was described in Yang *et al*. (2016). Construction of C-terminally Flag-tagged *Drosophila ERK(Rolled)-SBP* was described in Yang and Veraksa (2017). Construction of amino terminally tagged *HA-Raf*, and carboxy terminally tagged *MEK-V5* and *ERK-Flag* was described in Tipping *et al*. (2010). Site-directed mutagenesis was performed using the Q5 Site-Directed Mutagenesis Kit (New England BioLabs) on *pMT-ERK-Flag* following the manufacturer's protocol to generate $ERK^{Sem}$, $ERK^{H138A}$, and $ERK^{Sem/H138A}$, which were then subcloned into *pUAST-attB-SBP*. *Drosophila* S2 cells were used for all cell-based assays. Cells were cultured at 25°C in standard Schneider's S2 medium with 10% fetal bovine serum (Life Technologies) and 5% Pen/Strep (Invitrogen). For stable expression in S2 cells, a pMK33-Cic-SBP construct was transfected by using Effectene transfection reagent (Qiagen), and stable cell lines were selected in the presence of 300 µg/ml hygromycin (Sigma). Transient DNA transfections were performed using Effectene transfection reagent (Qiagen). At 24 h after transfection with indicated plasmids, cells were induced with 0.35 mM $CuSO_4$ and incubated overnight to allow expression of the protein. Cells were harvested and then lysed with default lysis buffer (50 mM Tris, pH 7.5, 125 mM NaCl, 5% glycerol, 0.2% IGEPAL CA-630, 1.5 mM $MgCl_2$, 1 mM dithiothreitol, 25 mM NaF, 1 mM $Na_3VO_4$, 1 mM EDTA) containing 2x Complete protease inhibitor (Roche). Cleared cell lysates were incubated with anti-V5 beads (Sigma) or Streptavidin beads (Pierce) at 4°C for 2 h. Beads were washed three times with default lysis buffer, and the protein complexes were eluted with SDS sample buffer. Immunoprecipitations using Cic-Venus–expressing embryos followed a similar protocol using GFP-Trap beads (Chromotek). All experiments were carried out at least twice, and representative results are shown.

### Immunoblotting and immunostaining

Protein complexes were resolved on 8% SDS protein gels and transferred onto Millipore Immobilon-FL PVDF Transfer Membranes with 0.45-µm pores. Primary antibodies used for Western blots were as follows: mouse anti-dpERK 1:1000 (Sigma), rabbit anti–total ERK 1:1000 (Cell Signaling Technology), mouse anti-V5 1:1000 (Sigma), rabbit anti-Flag 1:1000 (Sigma), and mouse anti-SBP 1:1000 (Santa Cruz Biotechnology). Secondary antibodies used were as follows: IRDye 800CW donkey anti-rabbit immunoglobulin G (IgG) 1:20,000 (LI-COR) and IRDye 680CW donkey anti-mouse IgG, 1:20,000 (LI-COR). Primary antibodies used for S2 cell staining were as follows: mouse anti-dpERK 1:500 (Sigma), rabbit anti-V5 1:500 (Sigma), rabbit anti-Flag 1:500 (Sigma), and mouse anti–nonphosphorylated ERK 1:500 (Sigma). Secondary antibodies used were as follows: donkey anti-rabbit Alexa Fluor 488 1:500 (Invitrogen) and goat anti-mouse Alexa Fluor 555 1:500 (Invitrogen). Stained cells were mounted with Prolong Gold anti-fade mounting reagent with 4′,6-diamidino-2-phenylindole (Life Technologies), and images were acquired with Zeiss LSM 880 confocal microscope. Embryo staining was performed as in Lim *et al*. (2015). Rabbit antibody to total ERK (1:100 dilution) was used as primary antibody, Alexa Fluor 488 anti-rabbit conjugate (1:500 dilution; Invitrogen) or Alexa Fluor 568 anti-rabbit conjugate 1:500 (Invitrogen) was used as secondary antibody. All experiments were carried out at least twice, and representative results are shown. All statistical analyses were performed using Student's *t* test.

### Purification of unphosphorylated and phosphorylated ERK from bacteria

For the expression of ERK2, the plasmid encoding tagged rat ERK2 in pQE80 was transformed into *Escherichia coli* BL21(DE3)-competent cells. Overnight cultures were subcultured into 1 l LB (Luria–Bertani) medium supplemented with 100 µg/ml ampicillin to a starting $OD_{600}$ of 0.02, and cultures were grown at 37°C with agitation at 250 rpm until they reached an $OD_{600}$ of 1.0. Protein expression was induced with 1 mM isopropyl β-D-1-thiogalactopyranoside (IPTG) and cultures were grown at 22°C for 6 h with agitation at 250 rpm. Bacterial cell pellets were harvested by centrifugation and stored at –20°C. For the expression of phosphorylated ERK2 (dpERK2), the plasmids encoding tagged rat ERK2 in pQE80 and tagged constitutively active (CA)-MEK1 (MEK1-G7B; Mansour *et al*., 1996) in

pBAD33 were transformed into *E. coli* BL21(DE3)-competent cells. Overnight cultures were subcultured into 1 l LB medium supplemented with 100 µg/ml ampicillin and 25 µg/ml chloramphenicol to a starting $OD_{600}$ of 0.02, and cultures were grown at 37°C with agitation at 250 rpm. At an $OD_{600}$ of 0.8, 0.1% L-arabinose was added, and the temperature was shifted to 22°C. At $OD_{600}$ 1.0, ERK2 protein expression was induced with 1 mM IPTG, and cultures were grown at 22°C for 6 h with agitation at 250 rpm. Bacterial cell pellets were harvested by centrifugation and stored at –20°C. For all protein purifications, cell pellets were resuspended in 40 ml of 10 mM imidazole, 300 mM NaCl, and 50 mM $NaH_2PO_4$ (pH 8) and lysed by treatment with lysozyme and sonication on ice. Cell debris was removed by centrifugation, and the supernatant was sterile filtered. All proteins were purified from clarified lysate using Ni-NTA agarose resin (Qiagen) following the manufacturer's recommendations. ERK2 was buffer exchanged into 50 mM HEPES, 100 mM NaCl, 20 mM $MgCl_2$, and 10% glycerol (pH 7.4) using PD-10 desalting columns (Bio-Rad). Aliquots of 5–50 µl were snap frozen in liquid nitrogen and stored at –80°C.

### In vitro binding assays

S2 cells were transfected with *pMT-Cic-V5* or empty vector. Transfected cells were preincubated with 2 µM PD0325901, an MEK inhibitor (Biotang) with dimethyl sulfoxide as vehicle, for 3 h before induction. Cells were induced with 0.35 mM $CuSO_4$ and incubated overnight. Extracts prepared as described earlier (except additional IGEPAL was added to default lysis buffer for a final concentration of 0.4%), and were incubated with anti-V5 beads for 2 h at 4°C. After three washes, the Cic-V5-bound beads were incubated with 500 ng of purified ERK2 or dpERK2 in default lysis buffer for 2 h at 4°C. Bovine serum albumin was added in binding solution to the final concentration of 0.05%, to reduce nonspecific binding to the beads.

### *Drosophila melanogaster* stocks

Fly stocks and crosses were maintained on standard yeast–cornmeal–agar medium at 25°C or 18°C. *MS1096-GAL4* was from the Bloomington *Drosophila* Stock Center. *UAS-MEK$^{E203K}$*, *Histone-GFP*, and *P{matα4-GAL-VP16}67*, used as a maternal driver, were described in Goyal *et al.* (2017a). Wild-type *Drosophila* ERK (*rolled*) as well as ERK mutants, C-terminally tagged with SBP, were subcloned into *pUAST-attB*, and transgenic lines were generated by inserting the constructs into the *attP40* genomic site by using φC31-based integration system (Venken *et al.*, 2006; Bischof *et al.*, 2007). All constructs were sent for injection together and therefore provide a matching set for comparisons of expression levels. *Cic-Venus* uses genomic regulatory sequences for expression and was described in Grimm *et al.* (2012).

### Wing phenotypes

Transgenic male flies were crossed with *MS1096-GAL4* virgins, and the wings of the resulting female progeny were imaged with Olympus BX60 compound microscope using bright-field illumination and a 4× objective.

## ACKNOWLEDGMENTS

We thank the Bloomington *Drosophila* Stock Center and the Vienna *Drosophila* Resource Centre for their services. We are grateful to Gerardo Jimenez for fruitful discussions and comments on the article. This work was supported by National Institutes of Health grant HD085870 (to A.V. and S.Y.S.). L.Y. and S.P. were supported by a UMass Boston Sanofi Genzyme Doctoral Fellowship.

## REFERENCES

Adachi M, Fukuda M, Nishida E (1999). Two co-existing mechanisms for nuclear import of MAP kinase: passive diffusion of a monomer and active transport of a dimer. EMBO J 18, 5347–5358.

Ajuria L, Nieva C, Winkler C, Kuo D, Samper N, José Andreu M, Helman A, González-Crespo S, Paroush Z, Courey AJ, Jiménez G (2011). Capicua DNA binding sites are general response elements for RTK signaling in *Drosophila*. Development 138, 915–924.

Astigarraga S, Grossman R, Diaz-Delfin J, Caelles C, Paroush Z, Jimenez G (2007). A MAPK docking site is critical for downregulation of Capicua by Torso and EGFR RTK signaling. EMBO J 26, 668–677.

Bischof J, Maeda RK, Hediger M, Karch F, Basler K (2007). An optimized transgenesis system for *Drosophila* using germ-line-specific phi C31 integrases. Proc Natl Acad Sci USA 104, 3312–3317.

Bott CM, Thorneycroft SG, Marshall CJ (1994). The sevenmaker gain-of-function mutation in p42 MAP kinase leads to enhanced signalling and reduced sensitivity to dual specificity phosphatase action. FEBS Lett 352, 201–205.

Brunner D, Oellers N, Szabad J, Biggs WH 3rd, Zipursky SL, Hafen E (1994). A gain-of-function mutation in *Drosophila* MAP kinase activates multiple receptor tyrosine kinase signaling pathways. Cell 76, 875–888.

Burkhard KA, Chen F, Shapiro P (2011). Quantitative analysis of ERK2 interactions with substrate proteins: roles for kinase docking domains and activity in determining binding affinity. J Biol Chem 286, 2477–2485.

Canagarajah BJ, Khokhlatchev A, Cobb MH, Goldsmith EJ (1997). Activation mechanism of the MAP kinase ERK2 by dual phosphorylation. Cell 90, 859–869.

Capdevila J, Guerrero I (1994). Targeted expression of the signaling molecule decapentaplegic induces pattern duplications and growth alterations in *Drosophila* wings. EMBO J 13, 4459–4468.

Coppey M, Boettiger AN, Berezhkovskii AM, Shvartsman SY (2008). Nuclear trapping shapes the terminal gradient in the *Drosophila* embryo. Curr Biol 18, 915–919.

Fryer JD, Yu P, Kang H, Mandel-Brehm C, Carter AN, Crespo-Barreto J, Gao Y, Flora A, Shaw C, Orr HT, Zoghbi HY (2011). Exercise and genetic rescue of SCA1 via the transcriptional repressor Capicua. Science 334, 690–693.

Fukuda M, Gotoh Y, Nishida E (1997). Interaction of MAP kinase with MAP kinase kinase: its possible role in the control of nucleocytoplasmic transport of MAP kinase. EMBO J 16, 1901–1908.

Futran AS, Kyin S, Shvartsman SY, Link AJ (2015). Mapping the binding interface of ERK and transcriptional repressor Capicua using photocrosslinking. Proc Natl Acad Sci USA 112, 8590–8595.

Futran AS, Link AJ, Seger R, Shvartsman SY (2013). ERK as a model for systems biology of enzyme kinetics in cells. Curr Biol 23, R972–R979.

Gabay L, Seger R, Shilo BZ (1997). MAP kinase in situ activation atlas during *Drosophila* embryogenesis. Development 124, 3535–3541.

Goyal Y, Jindal GA, Pelliccia JL, Yamaya K, Yeung E, Futran AS, Burdine RD, Schupbach T, Shvartsman SY (2017a). Divergent effects of intrinsically active MEK variants on developmental Ras signaling. Nat Genet 49, 465–469.

Goyal Y, Levario TJ, Mattingly HH, Holmes S, Shvartsman SY, Lu H (2017b). Parallel imaging of *Drosophila* embryos for quantitative analysis of genetic perturbations of the Ras pathway. Dis Model Mech 10, 923–929.

Grimm O, Sanchez Zini V, Kim Y, Casanova J, Shvartsman SY, Wieschaus E (2012). Torso RTK controls Capicua degradation by changing its subcellular localization. Development 139, 3962–3968.

Jacobs D, Glossip D, Xing H, Muslin AJ, Kornfeld K (1999). Multiple docking sites on substrate proteins form a modular system that mediates recognition by ERK MAP kinase. Genes Dev 13, 163–175.

Jimenez G, Guichet A, Ephrussi A, Casanova J (2000). Relief of gene repression by Torso RTK signaling: role of capicua in *Drosophila* terminal and dorsoventral patterning. Genes Dev 14, 224–231.

Jimenez G, Shvartsman SY, Paroush Z (2012). The Capicua repressor—a general sensor of RTK signaling in development and disease. J Cell Sci 125, 1383–1391.

Jin Y, Ha N, Fores M, Xiang J, Glasser C, Maldera J, Jimenez G, Edgar BA (2015). EGFR/Ras signaling controls *Drosophila* intestinal stem cell proliferation via Capicua-regulated genes. PLoS Genet 11, e1005634.

Johnson HE, Goyal Y, Pannucci NL, Schupbach T, Shvartsman SY, Toettcher JE (2017). The spatiotemporal limits of developmental Erk signaling. Dev Cell 40, 185–192.

Karim FD, Rubin GM (1999). PTP-ER, a novel tyrosine phosphatase, functions downstream of Ras1 to downregulate MAP kinase during *Drosophila* eye development. Mol Cell 3, 741–750.

Kim Y, Coppey M, Grossman R, Ajuria L, Jimenez G, Paroush Z, Shvartsman SY (2010). MAPK substrate competition integrates patterning signals in the *Drosophila* embryo. Curr Biol 20, 446–451.
Kim Y, Paroush Z, Nairz K, Hafen E, Jiménez G, Shvartsman SY (2011). Substrate-dependent control of MAPK phosphorylation in vivo. Mol Syst Biol 7, 467.
Lam YC, Bowman AB, Jafar-Nejad P, Lim J, Richman R, Fryer JD, Hyun ED, Duvick LA, Orr HT, Botas J, Zoghbi HY (2006). ATAXIN-1 interacts with the repressor Capicua in its native complex to cause SCA1 neuropathology. Cell 127, 1335–1347.
Lee T, Hoofnagle AN, Kabuyama Y, Stroud J, Min X, Goldsmith EJ, Chen L, Resing KA, Ahn NG (2004). Docking motif interactions in MAP kinases revealed by hydrogen exchange mass spectrometry. Mol Cell 14, 43–55.
Lemmon MA, Schlessinger J (2010). Cell signaling by receptor tyrosine kinases. Cell 141, 1117–1134.
Lim B, Dsilva CJ, Levario TJ, Lu H, Schupbach T, Kevrekidis IG, Shvartsman SY (2015). Dynamics of inductive ERK signaling in the *Drosophila* embryo. Curr Biol 25, 1784–1790.
Lim B, Samper N, Lu H, Rushlow C, Jimenez G, Shvartsman SY (2013). Kinetics of gene derepression by ERK signaling. Proc Natl Acad Sci USA 110, 10330–10335.
Löhr U, Chung H-R, Beller M, Jäckle H (2009). Antagonistic action of Bicoid and the repressor Capicua determines the spatial limits of *Drosophila* head gene expression domains. Proc Natl Acad Sci USA 106, 21695–21700.
Mansour SJ, Candia JM, Matsuura JE, Manning MC, Ahn NG (1996). Interdependent domains controlling the enzymatic activity of mitogen-activated protein kinase kinase 1. Biochemistry 35, 15529–15536.
Molnar C, de Celis JF (2013). Tay bridge is a negative regulator of EGFR signalling and interacts with Erk and Mkp3 in the *Drosophila melanogaster* wing. PLoS Genet 9, e1003982.
Roch F, Jiménez G, Casanova J (2002). EGFR signalling inhibits Capicua-dependent repression during specification of *Drosophila* wing veins. Development 129, 993–1002.
Ronchi E, Treisman J, Dostatni N, Struhl G, Desplan C (1993). Down-regulation of the *Drosophila* morphogen bicoid by the torso receptor-mediated signal transduction cascade. Cell 74, 347–355.
Roskoski R Jr (2012). ERK1/2 MAP kinases: structure, function, and regulation. Pharmacol Res 66, 105–143.
Sharrocks AD, Yang SH, Galanis A (2000). Docking domains and substrate-specificity determination for MAP kinases. Trends Biochem Sci 25, 448–453.
Simon-Carrasco L, Grana O, Salmon M, Jacob HKC, Gutierrez A, Jimenez G, Drosten M, Barbacid M (2017). Inactivation of Capicua in adult mice causes T-cell lymphoblastic lymphoma. Genes Dev 31, 1456–1468.
Suisse A, He D, Legent K, Treisman JE (2017). COP9 signalosome subunits protect Capicua from MAPK-dependent and -independent mechanisms of degradation. Development 144, 2673–2682.
Tan Q, Brunetti L, Rousseaux MWC, Lu HC, Wan YW, Revelli JP, Liu Z, Goodell MA, Zoghbi HY (2018). Loss of Capicua alters early T cell development and predisposes mice to T cell lymphoblastic leukemia/lymphoma. Proc Natl Acad Sci USA 115, E1511–E1519.
Tanaka M, Yoshimoto T, Nakamura T (2017). A double-edged sword: the world according to Capicua in cancer. Cancer Sci 108, 2319–2325.
Tanoue T, Adachi M, Moriguchi T, Nishida E (2000). A conserved docking motif in MAP kinases common to substrates, activators and regulators. Nat Cell Biol 2, 110–116.
Tipping M, Kim Y, Kyriakakis P, Tong M, Shvartsman SY, Veraksa A (2010). β-arrestin Kurtz inhibits MAPK and Toll signaling in *Drosophila* development. EMBO J 29, 3222–3235.
Tseng AS, Tapon N, Kanda H, Cigizoglu S, Edelmann L, Pellock B, White K, Hariharan IK (2007). Capicua regulates cell proliferation downstream of the receptor tyrosine kinase/ras signaling pathway. Curr Biol 17, 728–733.
Venken KJ, He Y, Hoskins RA, Bellen HJ (2006). P[acman]: a BAC transgenic platform for targeted insertion of large DNA fragments in *D. melanogaster*. Science 314, 1747–1751.
von Kriegsheim A, Baiocchi D, Birtwistle M, Sumpton D, Bienvenut W, Morrice N, Yamada K, Lamond A, Kalna G, Orton R, *et al*. (2009). Cell fate decisions are specified by the dynamic ERK interactome. Nat Cell Biol 11, 1458–1464.
Yang L, Paul S, Trieu KG, Dent LG, Froldi F, Fores M, Webster K, Siegfried KR, Kondo S, Harvey K, *et al*. (2016). Minibrain and wings apart control organ growth and tissue patterning through down-regulation of Capicua. Proc Natl Acad Sci USA 113, 10583–10588.
Yang L, Veraksa A (2017). Single-step affinity purification of ERK signaling complexes using the streptavidin-binding peptide (SBP) tag. Methods Mol Biol 1487, 113–126.